CLUSTERING INVERSE BEAMFORMING FOR INTERIOR SOUND SOURCE LOCALIZATION: APPLICATION TO A CAR CABIN MOCK-UP

Claudio Colangeli[1], Paolo Chiariotti[2], Gianmarco Battista[2], Paolo Castellini[2] and Karl Janssens[1]

[1]Siemens Industry Software NV
Interleuvenlaan 68, 3001, Leuven, Belgium
[2]Università Politecnica delle Marche
Via Brecce Bianche 1,60131, Ancona, Italy

ABSTRACT

Interior noise evaluation is a crucial aspect in NVH. The capability of correctly identifying and tackling noise problems that directly affect the passengers' experience in vehicle cabins is becoming more and more important in both the automotive and the aeronautic industry. Interior beamforming techniques play an important role in this context. However, their performances are limited by the complexity of the acoustic field in cabins. For this reason, despite the interesting solutions available (e.g. rigid spherical arrays, accurate models of the cavity, etc.), interior beamforming has been so far mainly limited to troubleshooting applications. The ambition is to go further, which means obtaining reliable quantitative results, increasing the achievable dynamic range and reducing the inaccuracy due to the complex phenomena taking place in a closed envelope. In this paper the Clustering Inverse Beamforming technique is applied for the first time in interior noise source identification problems. A new formulation adopting a 3D array of microphones randomly distributed in the cavity is presented. Experimental results are presented in a car cabin mock-up.

1   INTRODUCTION

 In-vehicle Sound Source Localization (SSL) is gaining more and more importance in NVH, since a correct identification of the noise sources represents the first step towards the improvement of the acoustic experience of a passenger. This paper introduces a novel inverse beamforming approach that aims at improving source localization and identification accuracy in closed cavities as car cabins. The approach bases on an evolution of the Clustering Inverse Beamforming formulation, which was firstly presented by Colangeli et al. in [1]. The new formulation aims at improving results in interior testing applications, even though a generalization to exterior problems and to different array geometries is straightforward.

Indeed the performance of a SSL technique is spoiled by the complexity of the acoustic field characterizing the vehicle cabin. Taking into account complex phenomena like multiple reflections, acoustic and vibro-acoustic modes represents a difficult task, and very often free-field conditions are assumed in SSL algorithms. However, such a simplified assumption might drastically decrease the accuracy of results in terms of both localization and identification. Many solutions have been proposed during the last years to tackle this issue. For instance, Castellini [2] proposed to reduce the effect of reflections by measuring with the microphone array placed in different positions inside the cabin and then by combining the beamforming output obtained from the processing of each measurement position. The approach assumes that reflections pattern identified by the array differs from position to position, while the actual source pattern remains constant. By combining results of the different tests, reflections fade out while actual sources are enhanced. Stationarity of the acoustic field is of course the main requirement for the exploitability of the method. Pereira [3] suggested to improve the SSL performance in enclosed spaces by extending the Equivalent Source method (ESM) formulation [4,5] to interior problems and coupling it to spherical arrays.

The approach presented in this paper can be seen as both an alternative and a complement to the aforementioned methods. Indeed the robustness of the Clustering Inverse Beamforming makes the approach suitable also for interior testing despite a free field radiation model is assumed. Moreover, the method is versatile and can be exploited with different array geometries, even though some benefits can be achieved in vehicle cabins with a distributed microphone configuration.

The paper is structured as follows. The Clustering Inverse Beamforming formulation will be presented in Section 2. The test set-up and the measurement matrix of the experiment will be discussed in Section 3. Section 4 will present the main results of the paper. In particular, a comparison between the use of Clustering Inverse Beamforming on a rigid spherical array and on a distributed array will be presented; an evolution of the algorithm will be introduced and the main results obtained using this new approach will also be shown. Section 5 will report the main conclusions of the work.

2   CLUSTERING INVERSE BEAMFORMING

The Clustering Inverse Beamforming (CIB) approach is a processing strategy that combines different clusters of microphones belonging to the same array in order to enhance the solution of an inverse beamformer. Indeed, the solution obtained by an inverse beamforming algorithm is strongly dependent on the combination of input available for retrieving the equivalent source distribution at the calculation points. By changing this set of input (i.e. considering different sub-sets of microphones in the inverse beamforming calculation), numerical instabilities, as well as phenomena not directly related to the source distributions (e.g. cavity modes), will be interpreted differently, while the actual noise sources will be identified similarly.

So far the approach exploits the Generalized Inverse Beamforming (GIB) approach [6,7,8], but the concept can be extended to different algorithms.

In GIB the source distribution is recovered by first decomposing the acoustic field in eigenmodes and then by solving, for each eigenmode, the general radiation problem reported in Eq. (1)

$$a_i = A^{-1}v_i = \Upsilon(A, v_i) \quad . \tag{1}$$

The following symbolism is adopted in (1):

- A: radiation matrix whose elements describe the radiation model adopted; in case of free-field propagation, each element of the A matrix can be expressed as

$$A_{mn} = \frac{e^{-ikr_{mn}}}{4\pi r_{mn}}$$

  where the subscripts m and n represent the mth microphone (over M) and n^{th} calculation point (over N) respectively and r_{mn} represents the distance between the geometrical positions of these two points;

- v_i: i^{th} eigenmode obtained from the Eigenvalue Decomposition of the microphone Cross Spectral Matrix ($C_M = ESE^{\dagger} \Rightarrow v_i = E\sqrt{S}$);

- a_i: reconstructed source distribution;

- Υ: operator taking into account regularisation strategy needed to cope with ill-the conditioning of the inverse problem and an iterative process for optimising the solution.

In GIB an iterative process that discards the weakest equivalent sources and recalculates the inversion of the problem considering only the remaining equivalent sources is adopted. This strategy aims at reducing the ill posedness of the problem by reducing the dimension of the radiation matrix. Numerical issues and ghost images are thus dramatically reduced and the dynamic range achievable can be considerably increased.

The Clustering approach consists in performing, per eigenmode, the inverse beamforming iterative process N_c times on N_c different clusters of microphones. Considering a subset – cluster - of microphones among those constituting the whole array means selecting only certain rows of the radiation matrix A, and thus changing the mathematical formulation of the problem. However, the associated physical event remains obviously the same. The regularisation strategies and the iterative solution of the inverse problem (the interested reader might refer to [8] for a deeper insight about regularisation strategies and sensitivity analysis in GIB) will perform differently depending on the radiation matrix considered. In this way, any numerical instability that gives rise to ghost sources will vary, while the actual sources will be constantly identified. The set of solutions obtained in this way ($a_c^{(i)}, c = 1: N_c$) for each ith main eigenmode (principal component), are processed in order to obtain a so-called *clustering mask matrix* ($\gamma^{(i)}$). In its current formulation, the *clustering mask matrix* is obtained by vector multiplying (Hadamard product) two matrices: the *normalised mean matrix* ($\bar{a}^{(i)}$) and the *normalised occurrences matrix* ($\hat{a}^{(i)}$).

The first one is obtained by averaging, per principal components, the set of solutions $a_c^{(i)} = \Upsilon(\{A\}_{c,N}, v_i)$ obtained processing each cluster of microphones over the N target points. The mathematical formulation of the normalised mean matrix is reported in Eq. (2).

$$\bar{a}^{(i)} = \frac{\sum_{c=1}^{Nc} a_c^{(i)}}{max\left(\sum_{c=1}^{Nc} a_c^{(i)}\right)} \tag{2}$$

The *normalised occurrences matrix* is obtained from the matrix $\breve{a}_c^{(i)}$ whose k^{th} element $(k = 1 : N)$ is defined as

$$\begin{cases} \breve{a}_c^{(i)}(k) = 1 \ if \ a_c^{(i)}(k) \neq 0 \\ \breve{a}_c^{(i)}(k) = 0 \ if \ a_c^{(i)}(k) = 0 \end{cases} . \tag{3}$$

Equation (3) gives the possibility to calculate the *normalised occurrences matrix* using Eq. (4) and Eq. (5)

$$\breve{a}^{(i)}(k) = \sum_{c=1}^{Nc} \breve{a}_c^{(i)}(k) \tag{4}$$

$$\hat{a}^{(i)} = \frac{\breve{a}^{(i)}}{max(\breve{a}^{(i)})} \tag{5}$$

Each element $\gamma^{(i)}(k)$ of the *clustering mask matrix* is calculated as

$$\gamma^{(i)}(k) = \bar{a}^{(i)}(k)\hat{a}^{(i)}(k) \tag{6}$$

and therefore the Clustering Inverse Beamforming solution can be obtained as

$$a^{(i)} = f(\Upsilon(A, v_i), \gamma^{(i)}) . \tag{7}$$

The process is summarized in Fig. 1 for a generic random array.
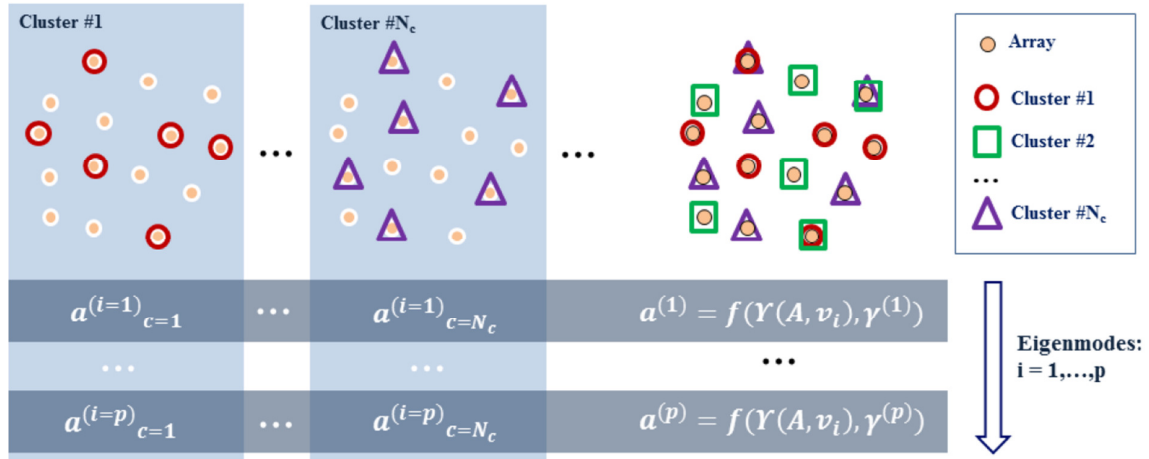
Fig. 1. Schematic description of the Clustering Inverse Beamforming approach

The function expressed in Eq. (7) can be shaped in several ways, among which the simplest involves the Hadamard product between the GIB solution matrix (estimated using the whole set of microphones) and the clustering mask matrix (8).

$$a^{(i)}(k) = a_i(k)\gamma^{(i)}(k) , k = 1, \dots, N \tag{8}$$

In this case, since each element of the clustering mask matrix ranges between 0 and 1, and it is greatest in correspondence of the sources locations, Eq. (8) will enhance localization of the actual sources, while suppressing any numerical instability and therefore increasing the dynamic of the solution retrieved.

The Clustering Inverse Beamforming can be addressed among the Bayesian approaches [9,10] in the sense that the solution of the whole inverse acoustic problem is improved on the basis of additional information linked to a statistical processing of multiple clusters of problems addressing the same physical event.

3   TEST CAMPAIGN

In order to prove the applicability of the clustering approach for enhancing interior beamforming results, a test campaign has been carried out on a simplified car cabin mock-up adopting a distributed microphone array. A test with a rigid spherical array was also carried out in order to prove the applicability of CIB to different array geometries. The entire test-rig has been set up into a semi-anechoic room, as visible in Fig. 2, in order to avoid any further influence from the surrounding environment.

| (a) | (b) |

Fig. 2. A picture of the car cabin mock-up with trimming material attached to the walls: (a) distributed and (b) spherical array

The car cabin mock-up consists of an aluminium frame (length × width × max-height : 1.450m×0.950m×0.700m) filled in with panels of different material: wood for the bottom panel, steel for the front vertical panel and PMMA (Polymethyl Methacrylate) for the rest of the panels. The trimming layers are removable and consist of pyramidal-shaped (0.045m×0.045m×0.060m) absorbing foam (density: 21 kg/m^3).

Two microphone arrays were tested: a distributed array and a rigid spherical array.

The former consists of 43 microphones randomly distributed over a frame made of aluminium rods and plastic wires. The array shape does not spoil its acoustic transparency in the frequency range 300 Hz – 10 kHz (frequency range of interest). The position of the microphones was randomized adopting two constraints: distance between microphones greater than 0.1m; distance of all the microphones from the panels greater than 0.05 m. The spherical array hosts 40 microphones distributed on a rigid sphere of diameter 0.20 m. The locations of microphones belonging to the two arrays with respect to the mock-up are reported in Fig. 3. Despite challenging, the identification of microphones locations inside a car cabin has been proved to be feasible in recent papers [11,12]. The higher geometrical complexity in dealing with a distributed array than with a spherical array can therefore be overcome using these strategies.
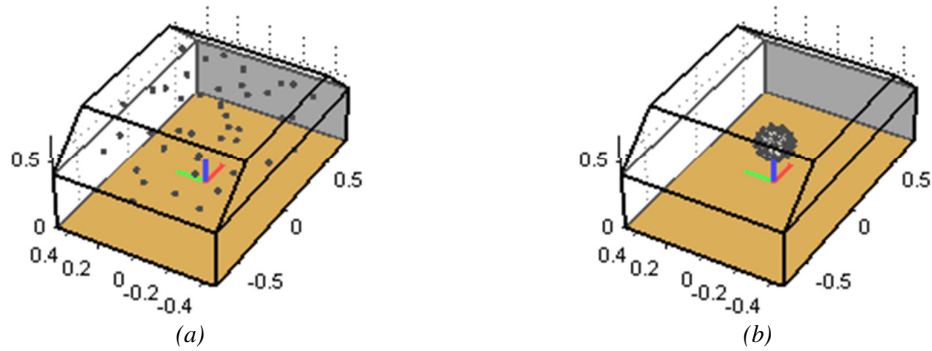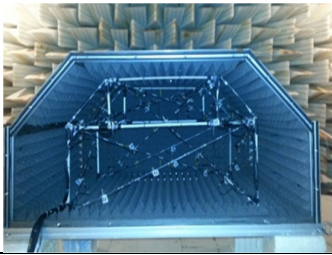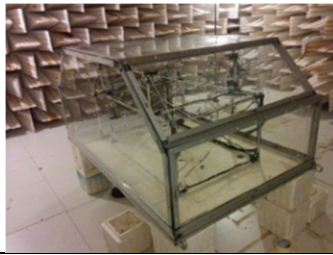
(a)   *(b)*

Fig. 3. Microphone locations with respect to the car mock-up: (a) distributed and (b) spherical array

Table 1. Car cabin mock-up (a) in the three configurations tested

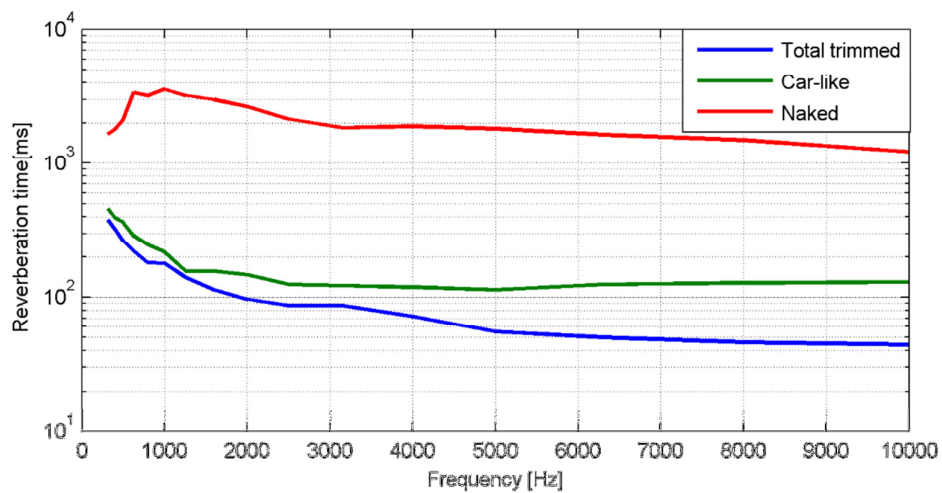| Total trimmed	Car-like	Naked
$\zeta = 100\ \%$	$\zeta = 73.9\ \%$	$\zeta = 0\ \%$

*Fig. 4. Mock-up reverberation time (T30) estimated for the three configurations tested*

The mock-up has been tested under three different configurations, as depicted in Table 1. The indicator ζ describes the percentage of the trimmed surface with respect to the total surface of the mock-up. The purpose of investigating these configurations was to test CIB in acoustic fields ranging from a free-field like (*Total Trimmed*) to a diffuse-field like (*Naked*)

6

configuration. A configuration resembling a car cabin (*Car-like*) was also tested. All these aspects well reflect in the values of reverberation time (T30 - Fig. 4) measured in the three configurations. As expected, the reverberation time is dramatically higher in the *Naked* configuration with respect to the two other cases. It is very interesting to notice that reverberation time is almost the same up to around 1500 Hz in the *Total trimmed* and *Car-like* configurations, while for higher frequencies the absorption properties of the trimming panels plays a more evident role.

Three different source scenarios were tested in each configuration (Table 2). A source position with respect to the mock-up is also reported in the picture at the bottom of the same table.

Table 2. Description of the tested scenarios (source position)

Scenario	Name	Position w.r.t. mock-up
a	Right panel, front bottom	Inside
b	Top panel, front middle	Outside
c	Left panel, front	Outside
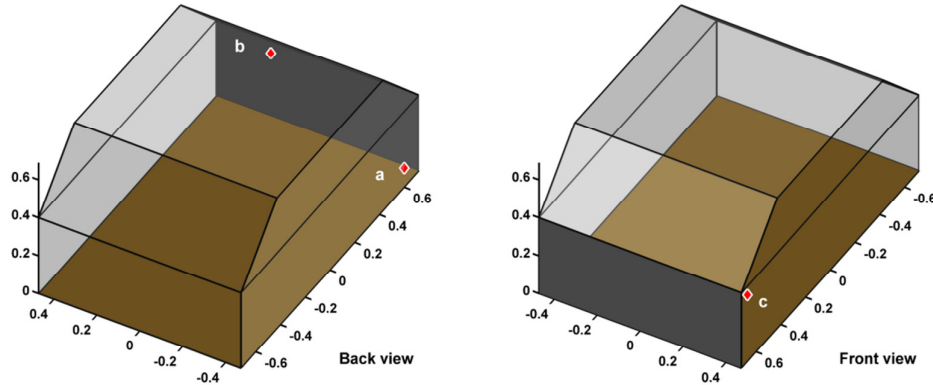
When the source is placed outside, noise is radiated towards the interior through the panels and panels also act as noise sources. When the source is placed inside the mock-up, mainly the acoustic and geometrical properties of the cavity come into play. LMS mid-high frequency

Q Source was used for generating white noise in the bandwidth 300 Hz – 10 kHz.

4   RESULTS

4.1   Clustering Inverse Beamforming on spherical and distributed arrays

The current standard in interior beamforming applications is to use a rigid sphere. However, the spherical harmonic expansion formulation, on which both direct and inverse methods dealing with scattering arrays are based, and the diameter of the sphere might limit the frequency range. There exist both "hardware-based" [13,14] and "software-based" [15] methods to cope with low-frequency extension. However, despite valuable, these methods have drawbacks mainly linked to the dimension of the acoustic cavity wherein the test has to

be carried out. The closeness of the hardware/software microphones to the walls of the cavity might seriously affect the accuracy of the approach.

A distributed array, i.e. an array with microphones randomly distributed inside the cavity, does not suffer of such low frequency issues. Moreover, its random nature matches perfectly with CIB.

This holding, the main results of the test campaign will be presented referring to the distributed array. However, for sake of completeness and to demonstrate the versatility of CIB, some results using the rigid spherical array are presented as well in the following.

Clusters of microphones, being subsets of the microphone array, can be selected randomly or under certain constraints. The parameters reported in Table 3 have been adopted for the spherical and the distributed array. A random choice of microphones belonging to each cluster was performed in both cases.

Table 3. CIB parameters for spherical and distributed array

	Spherical Array	*Distributed Array*
Number of microphones in each cluster (N_m)	19	15
Number of clusters (N_c)	30	100

Results plotted hereafter will not be shown with a colour bar associated in order to leave maximum visibility to noise maps. However, values reported in the paper follow the criterion of Fig. 5, to which the reader is referred for a quantitative interpretation of results. In particular: the dynamic range of the inverse beamforming result is kept greater than 40 dB, while the colour bar of the mask matrix map ranges between 0 and 1.

Fig. 5. Colour code for (top) inverse beamforming results in terms of SPL (dB, $p_{ref} = 20\ \mu Pa$) and (bottom) CIB mask matrix.

Fig. 6 and Fig. 7 show results in the "Total trimmed" configuration for the "*a*" scenario, at 2.5 kHz for the spherical and distributed array respectively. Results of standard GIB are also reported for sake of completeness. It is interesting to notice that CIB provides better results than standard GIB. The noise source is well located in either cases, but higher dynamic range is obtained using CIB. Both the scattering sphere and the distributed array provide similar performance in terms of localization and quantification capabilities at 2.5 kHz. Moreover, it is interesting to notice that CIB greatly improves results on the rigid sphere. This is also an important goal achieved, since the CIB strategy can be really considered a ready to use solution in those applications of interior sound source localization already faced with scattering spherical arrays. The distributed array provide more accurate results in the low frequency range (500Hz), as can be seen in Fig. 8 and in Fig. 9. This was expected, since the relative dimensions of the cavity and the sphere did not allow to use any strategy to extend the spherical array performance to lower frequencies. The distributed array can therefore be thought as an alternative to the spherical one whenever solutions for extending the performance of the scattering sphere at lower frequency cannot be carried out.
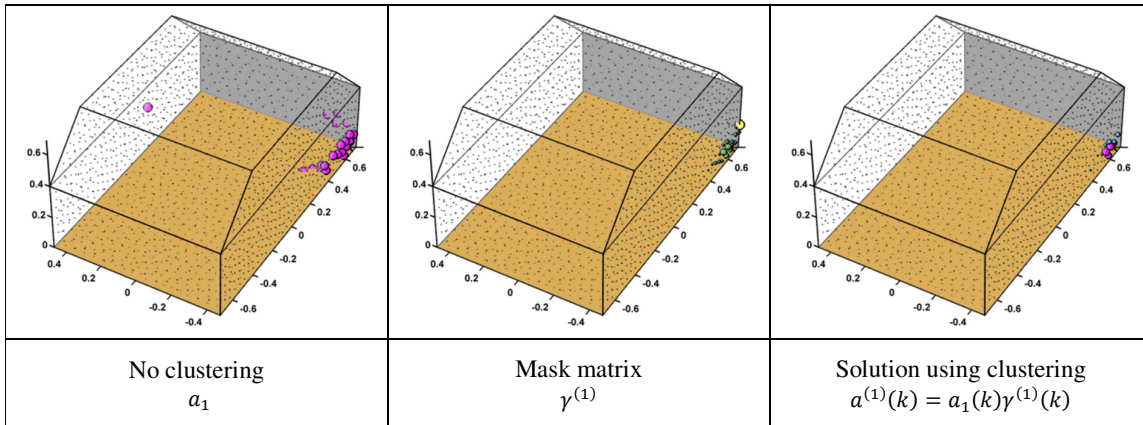
| No clustering a_1 | Mask matrix $\gamma^{(1)}$ | Solution using clustering $a^{(1)}(k) = a_1(k)\gamma^{(1)}(k)$ |

Fig. 6 CIB on Spherical array. Configuration: "Total trimmed". Scenario: a. Frequency: 2500 Hz

| No clustering a_1 | Mask matrix $\gamma^{(1)}$ | Solution using clustering $a^{(1)}(k) = a_1(k)\gamma^{(1)}(k)$ |

Fig. 7 CIB on Distributed array. Configuration: "Total trimmed". Scenario: a. Frequency: 2500 Hz

| No clustering a_1 | Mask matrix $\gamma^{(1)}$ | Solution using clustering $a^{(1)}(k) = a_1(k)\gamma^{(1)}(k)$ |

Fig. 8 CIB on Spherical array. Configuration: "Total trimmed". Scenario: a. Frequency: 500 Hz

No clustering a_1	Mask matrix $\gamma^{(1)}$	Solution using clustering $a^{(1)}(k) = a_1(k)\gamma^{(1)}(k)$
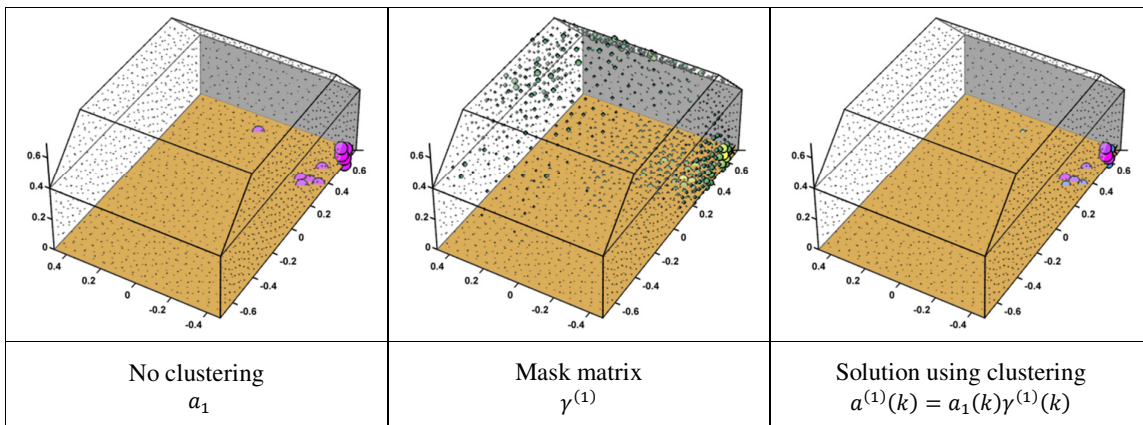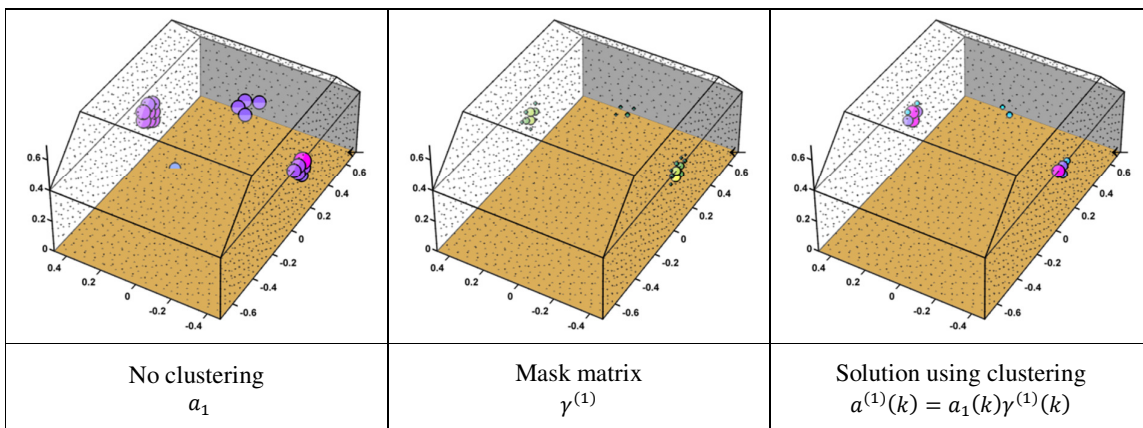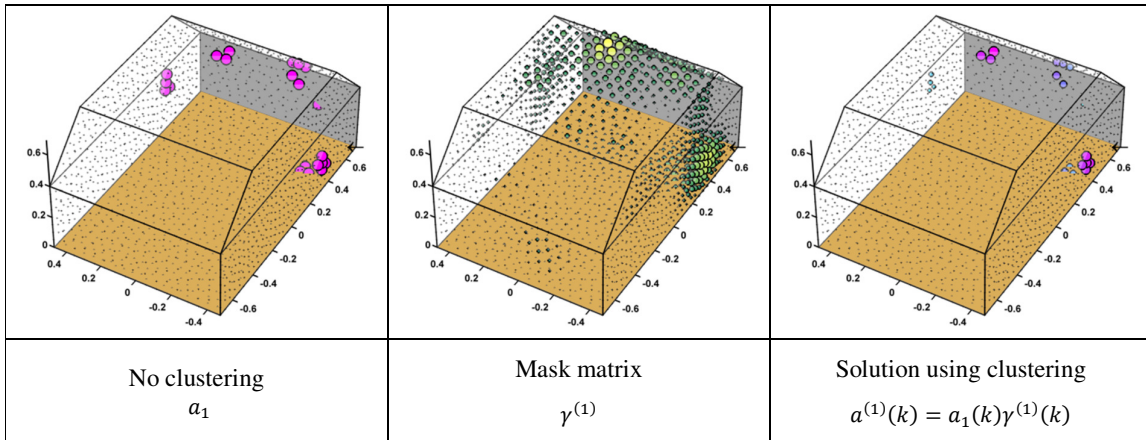
Fig. 9 CIB on Distributed array. Configuration: "Total trimmed". Scenario: a. Frequency: 500 Hz

4.2   Enhanced formulation of Clustering Inverse Beamforming

Although very powerful for enhancing the localization of the actual sources, Eq. 8 might reduce the accuracy in the quantification of the source strengths. A more accurate quantification might be obtained by adopting an alternative formulation of the f function in Eq. 7. Indeed, the information carried by the *clustering mask matrix $\gamma^{(i)}$* can be interpreted as a *Level of Confidence* (LoC) datum that gives an indication on how much a certain equivalent source distribution is representative of an actual source. The light of this assumption, the mask matrix can thus be exploited for selecting the subset of target grid points (N^*) complying with the condition reported in Eq. 9.

$$N^* = \{k, \qquad k \in 1, \dots, N, \qquad s.t.\ \gamma^{(i)} \geq LoC\} \qquad (9)$$

CIB can therefore be enhanced by using the *clustering mask matrix* to select those points to be used in the calculation of the GIB and by estimating the source distribution $a^{(i)}$ using the whole set of available microphones.

$$a^{(i)} = \Upsilon(\{A\}_{M,N^*}, v_i) \qquad (10)$$

A comparison demonstrating the enhanced performance of this approach with respect to the one addressed by Eq. 8 is reported in Fig. 10 and in Fig. 11. These figures refer also to two different acoustic fields taking place inside the cavity, a "free-field"-like one (the former) and a reverberant one (the latter). In both figures, Eq.10 is computed by previously putting to zero the mask matrix elements having values smaller than 0.5 (e.g. $\gamma^{(1)}(k) < LoC = 0.5, k = 1, \dots, N$).

The positive effects of this new CIB formulation is clearly visible on the two configurations reported: less numerical instabilities are present on the maps and higher dynamic range can be obtained. Moreover, it is interesting to report that, even though the free-filed assumption is not valid anymore in the "Naked" configuration, the new CIB formulation seems to partially cope with this without any change to the radiation model used. The localization of the source towards the rear inclined Plexiglas panel rather than on the corner might be due to the vibration of the panel induced by the source, since the source itself was placed outside the mock-up.
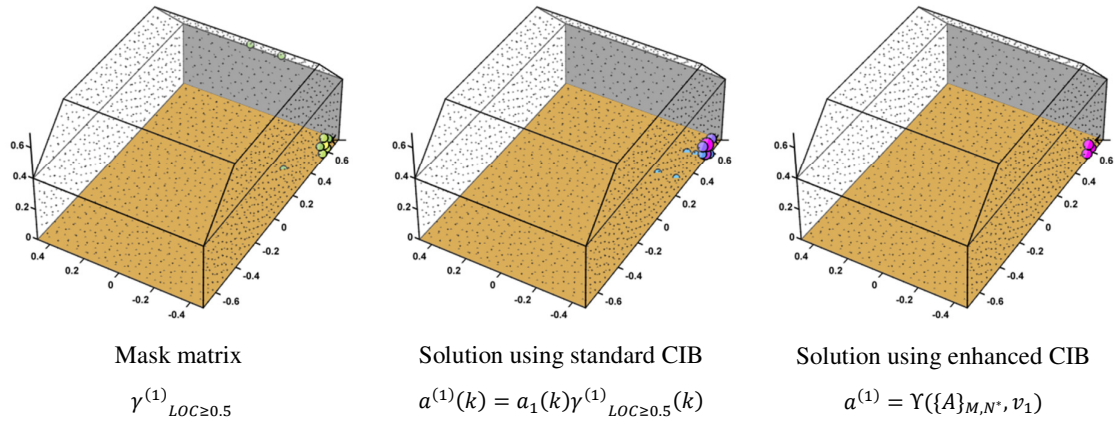
Mask matrix	Solution using standard CIB	Solution using enhanced CIB
$\gamma^{(1)}{}_{LOC \geq 0.5}$	$a^{(1)}(k) = a_1(k)\gamma^{(1)}{}_{LOC \geq 0.5}(k)$	$a^{(1)} = \Upsilon(\{A\}_{M,N^*}, v_1)$

Fig. 10. Use of the mask matrix with a set level of confidence (LoC). Configuration: "Total trimmed". Scenario: a. Frequency: 2300 Hz.

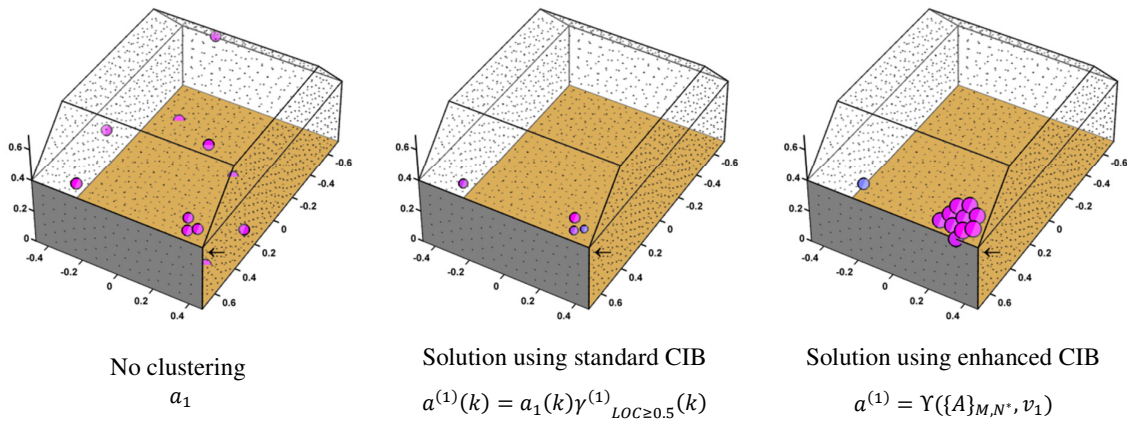| No clustering	Solution using standard CIB	Solution using enhanced CIB
a_1	$a^{(1)}(k) = a_1(k)\gamma^{(1)}{}_{LOC \geq 0.5}(k)$	$a^{(1)} = \Upsilon(\{A\}_{M,N^*}, v_1)$

Fig. 11. CIB applied in reverberant conditions. Configuration: "Naked". Scenario: c. Frequency: 500 Hz.

4.3   Results on the tested scenarios

Results presented hereafter aims at showing the performance of the enhanced CIB formulation on the distributed array at different frequency ranges for the three scenarios tested. The same settings reported in Table 3 were used in processing the data sets. Quantitative values are not reported due to the impossibility of comparing them to accurate reference values; however, dynamic range is always kept larger than 40 dB (SPL, p_{ref} = 20 μPa), coherently to Fig. 5.

The correct identification of noise sources in the low-frequency range is a challenging task. Indeed, the absorbing efficiency of the trimming material is poor below 1200 Hz (see Table 2), the wavelength of the acoustic waves in this frequency range is comparable with the three dimensions of the cavity, and therefore strong reflections and acoustic modes of the cavity may result not negligible, also in the "Total trimmed" scenario. These aspects are clearly visible in Fig. 12, where CIB results, in terms of mask matrices and CIB solutions, are reported for the frequency range 350-850Hz.
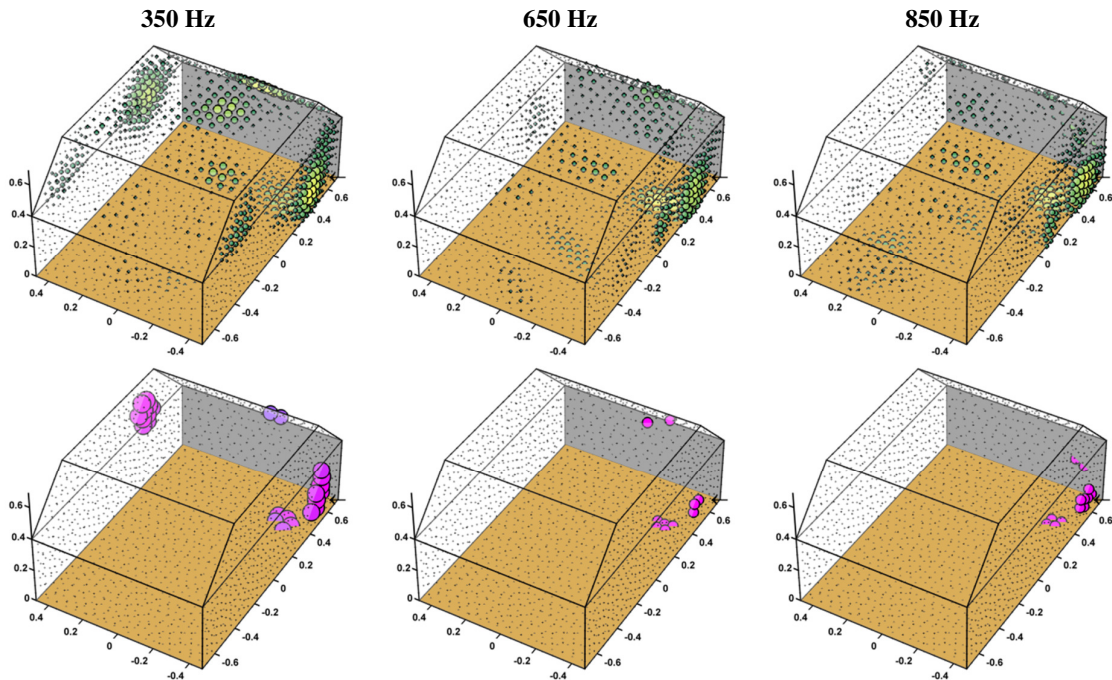
Fig. 12. Configuration: "Total trimmed". Scenario: a. Analysis of the solution at: 350 Hz – 850 Hz. Top: mask matrix $\gamma^{(1)}$. Bottom: solution using CIB $a^{(1)} = \Upsilon(\{A\}_{M,N^*}, v_1)$. Dynamic range: >40 dB.

Fig. 13 reports the results obtained by applying the proposed method the case of scenario *a* in the different configurations. Notice that it this particular scenario, the source is placed inside the cabin, therefore there is neither transmission through the cavity walls nor any excitation of the mock-up panels. However, strong reflections may take place. In the low frequency range, these reflections might appear even more relevant than the actual source. This is especially true for the "Naked" configuration.
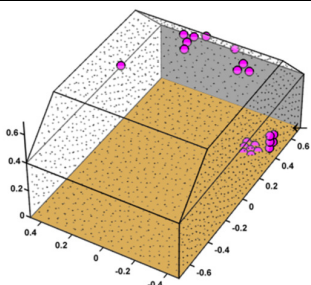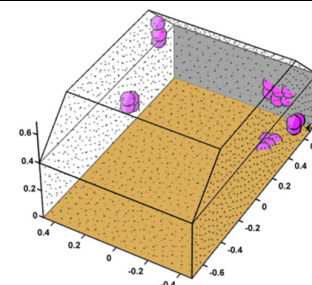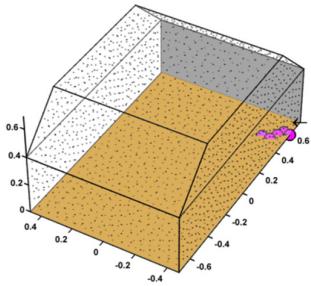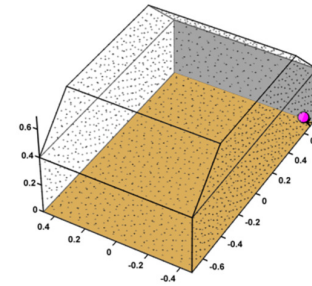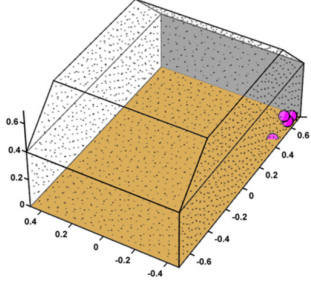
	Total trimmed	**Car-like**	**Naked**
500 Hz			/
2000 Hz			/
4000 Hz		Localization of the source successful up to 3500 Hz.	/

Fig. 13. CIB solutions for source Scenario: a, in all configuration tested. Dynamic range: >40 dB.

In Scenario *b* the source was place outside the mock-up. Results reported in Fig. 14 clearly highlight this source configuration turned out to provide better results in terms of localisation accuracy.
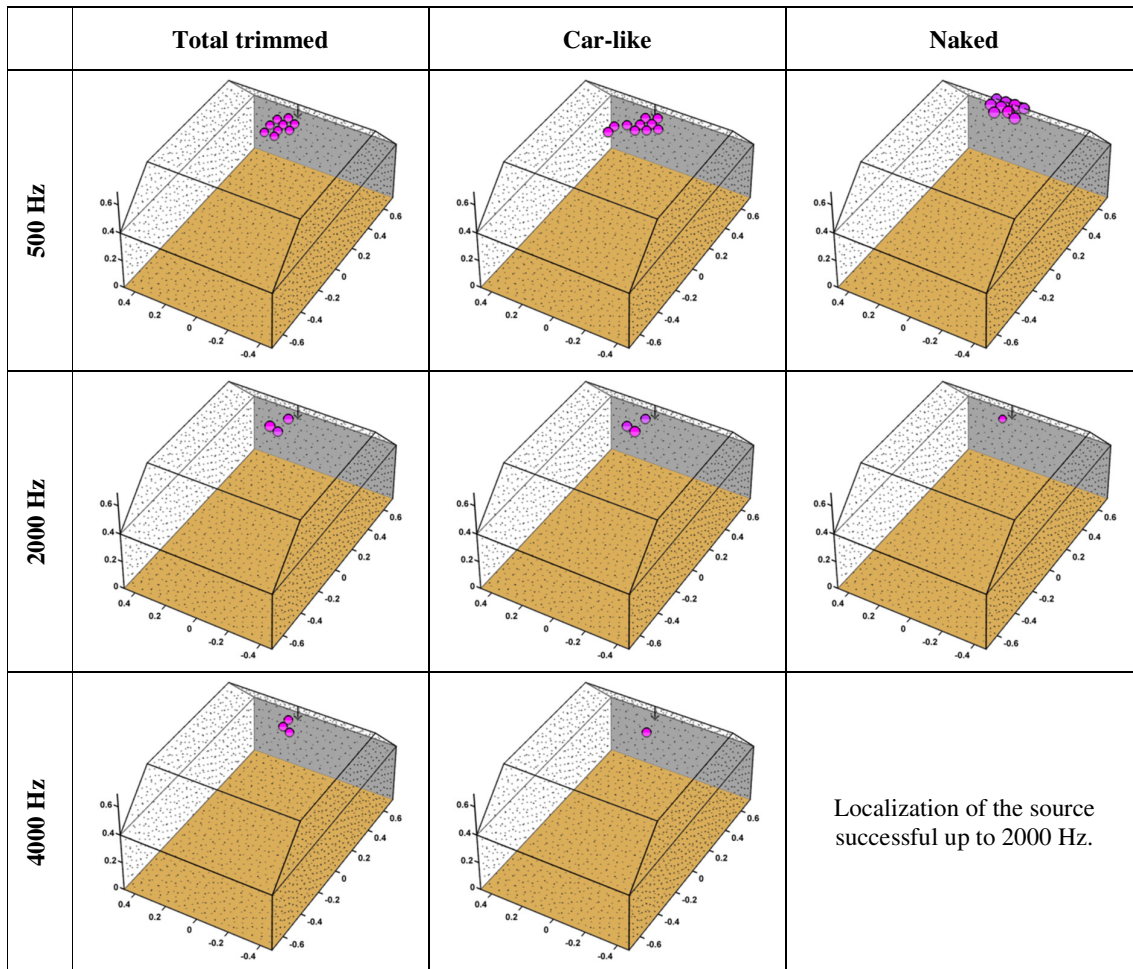

Fig. 14. CIB solutions for source Scenario: b, in all configuration tested. Dynamic range: >40 dB.

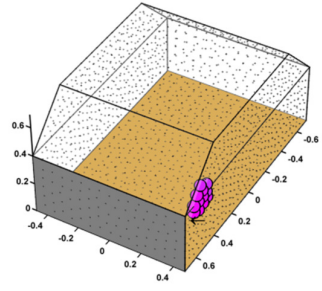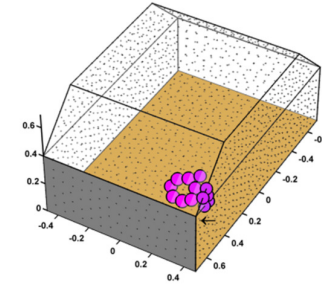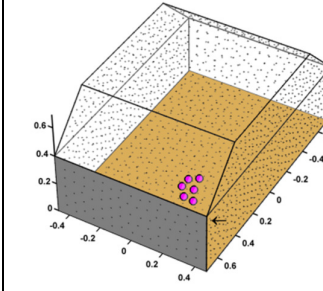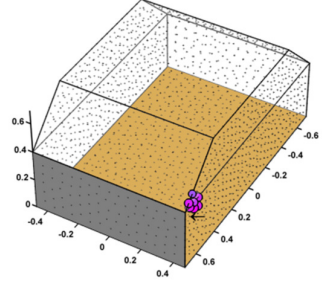The same trend can be noticed in Fig. 15 regarding results obtained for scenario *c*.

	Total trimmed	**Car-like**	**Naked**
500 Hz			
2000 Hz		Localization of the source successful up to 1400 Hz.	Localization of the source successful up to 500 Hz.
/	Localization of the source successful until 2000 Hz.	/	/

Fig. 15. CIB solutions for source Scenario: c, in all configuration tested. Dynamic range: >40 dB.

Table 4 – Applicability range of CIB for the three source scenarios and mock-up configurations.

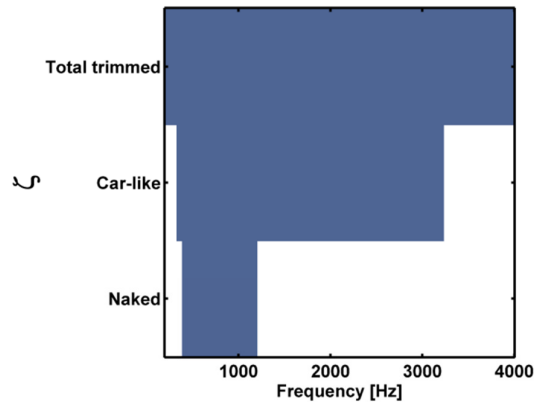|	Scenario "a"	Scenario "b"	Scenario "c"
Total trimmed	350 Hz – 4000 Hz	300 Hz – 4000 Hz	450 Hz – 2000 Hz
Car-like	350 Hz – 3500 Hz	300 Hz – 4000 Hz	450 Hz – 1400 Hz
Naked	/	300 Hz – 2000 Hz	450 Hz – 500 Hz

Table 4 summarises the frequency ranges wherein the noise source could be well localised for the three scenarios and mock-up configurations.

15

5   CONCLUSIONS

The paper presented an application of Clustering Inverse Beamforming to interior noise source identification problems. For the first time CIB was used on both scattering spherical array and distributed array, proving two main theses:

   a. CIB can be considered a ready to use formulation to be exploited in those noise source identification applications already faced with scattering spherical arrays;
   b. Distributed array might represent a valid alternative whenever it is not possible to extend the exploitability of the rigid spherical array (using either hardware or software solutions) to the low frequency range. Moreover, the distributed array might be useful for joint testing with Acoustic Modal Analysis applications.

An alternative formulation of CIB, wherein the clustering mask matrix of CIB is used as a Level of Confidence function for selecting the input target points of Generalized Inverse Beamforming, was also presented. This new formulation proved to provide more accurate results in terms of localization accuracy and dynamic range improvement.

The experimental tests performed on a scaled and simplified car cabin mock-up has highlighted the following aspects:

   - The proposed technique can be used (with different performances) also in reverberant conditions, without any change to the propagation model, only starting from a frequency that is dependent on the geometrical dimensions of the cabin;
   - To extend this frequency range to lower frequencies the propagation model adopted in the inverse beamforming formulation should be refined.

Authors are currently working to improve the robustness of the technique in real car environments and with multiple sources.

AKNOWLEDGEMENTS

REFERENCES

[1] C. Colangeli, P. Chiariotti, K. Janssens and P.Castellini. "A microphone clustering approach for improved Generalized Inverse Beamforming formulation." NOVEM Conference. Dubrovnik, Croatia, 2015.

[2] P. Castellini and A. Sassaroli. "Acoustic source localization in a reverberant environment by average beamforming." Mechanical Systems and Signal Processing, 24, 796-808, 2010.

[3] A. Pereira. "Acoustic imaging in enclosed spaces." PhD thesis 2013-ISAL-0066, INSA Lyon, 2013.

[4] G. H. Koopmann, L. Song, and J. B. Fahnline. "A method for computing acoustic fields based on the principle of wave superposition." The Journal of the Acoustical Society of America, vol. 86, no. 6, pp. 2433–2438, 1989

[5] R. Jeans and I. C. Mathews, "The wave superposition method as a robust technique for computing acoustic fields," The Journal of the Acoustical Society of America, vol. 92, no. 2, pp. 1156–1166, 1992

[6] T. Suzuki. "Generalized inverse beamforming algorithm resolving coherent/incoherent, distributed and multipole sources." AIAA/CEAS Aeroacoustics Conference, Vancouver, British Columbia Canada, 2008.

[7] P. Zavala, W. De Roeck, K. Janssens, J.R.F. Arruda, P. Sas and W. Desmet. "Generalized inverse beamforming with optimized regularization strategy." Mechanical Systems and Signal Processing, 25, 928-939, 2011.

[8] C. Colangeli, P. Chiariotti and K. Janssens. "Uncorrelated noise source separation using inverse beamforming." IMAC Conference. Orlando, Florida US, 2015.

[9] J. Antoni. "Bayesian vision of inverse acoustic problems." NOVEM Conference. Dubrovnik, Croatia, 2015.

[10] A. Pereira, Q. Leclére and J. Antoni. "A theoretical and experimental comparison of the equivalent source method and a Bayesian approach to noise source identification." Berlin Beamforming Conference, Berlin, Germany, 2012.

[11] G. Accardo, B. Cornelis, K. Janssens, and B. Peeters. "Automatic microphone localization inside a car cabin for experimental acoustic modal analysis." Proceedings of the 22nd International Congress on Sound and Vibration, Florence, Italy, 2015.

[12] G. Accardo, B. Cornelis, P. Chiariotti, K. Janssens, B. Peeters, and M. Martarelli. "A non-line-of-sight identification algorithm in automatic microphone localization for experimental acoustic modal analysis." Proceedings of the 44th International Congress on Noise Control Engineering, San Francisco, Californa, USA, 2015.

[13] A. Pereira, Q. Leclére, L. Lamotte, S. Paillasseur, L. Bleandonu, "Noise source identification in a vehicle cabin using an iterative weighted approach to the ESM method." ISMA Conference, Leuven, Belgium, 2012.

[14] L. Lamotte, O. Minck, S. Paillasseur. "Interior Noise Source Identification With Multiple Spherical Arrays In Aircraft And Vehicle", ICSV 20th, Bangkok, Thailand, 2013.

[15] E. Tiana-Roig, A. Torras-Rosell, E. Fernandez-Grande, C.H. Jeong, F.T. Agerkvist. "Enhancing the Beamforming map of Spherical Arrays at low frequencies using Acoustic Holography." Berlin Beamforming Conference, Berlin, Germany, 2014.